

Chapter 17

Smectic Phases of Liquid Crystalline Rod-Like Helical Polymers

Kento Okoshi

17.1 Introduction

In addition to the conventional liquid crystal molecules with aromatic mesogens and aliphatic tails, which are typically used in display devices, miscellaneous kinds of materials, i.e., DNA (Livolant and Bouligant 1986; Strzelecka et al. 1988a), viruses (Wen et al. 1989; Dozic and Fraden 1997; Adams et al. 1998; Lee et al. 2002, 2003), colloidal suspensions of crystal particles (Li et al. 2002; Gabriel et al. 2001), form liquid crystal phases even though they have different chemical properties. The common feature of these materials is their rod-shape (or disc shape) so that the long axis (or short axis when disc shaped) of the neighboring molecules can spontaneously align in a parallel manner. That is to say, the origin of liquid crystallinity is largely derived from the packing entropy of anisotropic shapes (excluded volume effect), thus it could be appropriate to evaluate them using physical models of rigid rod-like (or disc-like) particles.

These theoretical studies have been extensively performed both with numerical calculations and computer simulations to prove the entropically-driven liquid crystal formation, since the initial approach of Onsager's (Onsager 1949) and Flory's (Flory 1956) theoretical attempts to reproduce the nematic— isotropic transition. The series of studies blossomed into the reproduction of the most commonly observed liquid crystal phase sequence of the nematic—smectic—columnar phases of the monodisperse-length rigid-rod-like particle systems in the 1980s (Hosino et al. 1979, 1982; Stroobants et al. 1987; Veerman and Frenkel 1991; Bolhuis and Frenkel 1997), showing the possibility of an unexpected wide variety of liquid crystalline phases including the smectic phase in simple hard-rod systems.

K. Okoshi (✉)

Department of Bio- and Material Photonics, Chitose Institute of Science and Technology,
758-65 Bibi, Chitose, Hokkaido 066-8655, Japan
e-mail: k-okoshi@photon.chitose.ac.jp

It has also been shown that the gain in packing entropy exceeding the loss of translational entropy could be the major driving force of the liquid crystalline phase transition. Since then, these theoretical studies have centered on the lyotropic hard-rod systems with only entropy taken into consideration, and expanded from rod-like particles to disc-shaped (Veerman and Frenkel 1992), ellipsoidal (Frenkel et al. 1984), biaxial particles (Michael 1990), and mixtures, seemingly beyond the scope of the practical experimental verifications.

The detailed experimental verification of the theoretical predictions of the smectic phase in the simple hard-rod systems was first reported in biological systems because artificial systems are hardly ever truly monodispersed. The smectic phase and smectic—nematic lyotropic phase sequence in the aqueous dispersion of the tobacco mosaic virus (TMV) were determined in 1989 (Wen et al. 1989), followed by a number of studies on similar virus systems (Dozic and Fraden 1997; Adams et al. 1998; Lee et al. 2002, 2003). The monodispersed rod-like poly(γ -benzyl-L-glutamate) prepared by a bacterial synthetic method has also been reported to exhibit a smectic phase and twist grain boundary-like smectic phase in 1997 (Yu et al. 1997; He et al. 1998). However, it takes a very time-consuming and cost-intensive procedure to prepare the monodispersed polypeptide (Zhang et al. 1992), in which the bacterial protein expression of the artificial gene encoding the peptide sequence is followed by purification and benzylation of the product. Therefore, no further detailed experimental study on the smectic phase in the monodispersed polypeptide system has been performed, while all the other studies have been on viruses which are also not easy to handle.

17.2 Liquid Crystalline Phase Behavior of Rod-Like Polymers

17.2.1 Theoretical Predictions

The first indication of the most commonly observed liquid crystalline phase transition of smectic—nematic— isotropic in the rigid-rod particle systems was shown by the mean field approximation, in which the free energy of the rigid-rod particles described by a positional and orientational order is reduced to a minimum, as reported by Kimura et al. in 1979 (Hosino et al. 1979). Later, in 1987, the entire phase diagram versus the aspect ratio (ratio of length to diameter of the rod-like particle) and reduced volume density (defined as ρ/ρ_{CP} , where ρ_{CP} is the close packed density) of the rod-like particles has been revealed by computer simulations (Fig. 17.1a) (Stroobants et al. 1987), indicating that the columnar—smectic—nematic phase transition takes place (without isotropic phase due to the uniform alignment approximation), although the stability of the columnar phase was found to be susceptible to the system size of the simulation in a following study (Veerman

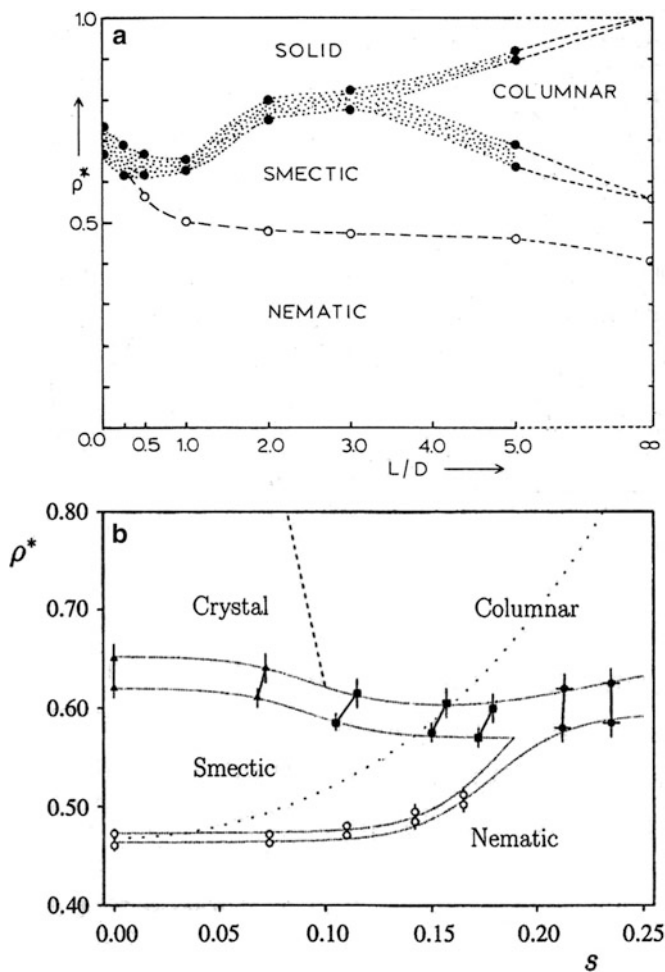


Fig. 17.1 Computed phase diagram of (a) monodisperse (Stroobants et al. 1987) and (b) polydisperse (Bates and Frenkel 1998) length hard parallel rod-like particle systems as a function of the aspect ratio and reduced volume density of the particles for (a), and polydispersity and reduced volume density of the particles for (b)

and Frenkel 1991). Interestingly, a similar result had been indicated only with the attractive potential taken into consideration in 1971 (Kobayashi 1970; McMillan 1971).

The rod-like particle systems with a length polydispersity have also been computed (Bates and Frenkel 1998) because further detailed experimental studies should be performed with easy-to-handle artificial rod-like polymer systems which inevitably possess a polydispersity. Figure 17.1b shows the phase diagram in the limit of the infinite aspect ratio drawn as a function of the polydispersity of the rod

length, s (standard deviation when the average length is unity) and reduced volume density. The smectic phase is increasingly destabilized compared to the nematic phase and depleted at $s = 0.18$ (which corresponds to $M_w/M_n = 1.03$, assuming the normal distribution.), although the phase behavior is almost the same as with the monodispersity for a low polydispersity, $0 < s < 0.08$. These results naturally lead us to the idea that even synthetic stiff polymers form a smectic phase when their polydispersity is quite narrow.

17.2.2 Experimental Verifications

The synthetic helical polymers are the most suitable for the experimental verification of these theoretical predictions because this group of polymers is stiff enough to be regarded as a rigid rod. The first clear finding of a smectic phase in the synthetic helical polymer system was achieved with a polysilane (poly-1 in Fig. 17.2a) (Okoshi et al. 2002a) which takes an exceptionally rigid helical conformation with the persistence length of 85 nm due to the severe restriction on the main chain conformation caused by the steric hindrance between the long and branched alkyl side chains (Fujiki 1996; Terao et al. 2001), although ambiguous indications of the smectic phase had been reported with DNA and a synthetic peptide based only upon polarized optical microscopic observations (Strzelecka et al. 1988b; Watanabe and Takashina 1992). The thermotropic smectic phases formed by poly-1, 2, 3 (Fig. 17.2a) have been intensively studied, even though these should be lyotropic systems to verify the theoretical predictions of the rigid-rod particle systems. This is because the long alkyl chain behaves as the solvent in the thermotropic system, and this makes it possible to avoid some experimental difficulties, such as solvent evaporation, phase separation, and sedimentation in the lyotropic solutions. Moreover, it is easy to narrow the molecular weight (molecular length) distributions of poly-1, 2, 3 to such an extent that M_w/M_n is approximately 1.1 by simple solvent fractionation because there is little polymer aggregation in the nonpolar solvent due to the nonpolar and stiff (rod-like) nature of the polysilanes. As predicted, the thermotropic liquid crystalline phase behavior of poly-1, 2, 3 strongly depends on the polydispersity of their molecular weight, as it shows a nematic (cholesteric) phase when its M_w/M_n is high, while it shows a smectic phase when its M_w/M_n is low (Okoshi et al. 2002a).

Figures 17.2b–d show the polarized optical micrograph of poly-1 and small- and wide-angle X-ray scattering patterns of the oriented sample of poly-3 with a narrow molecular weight distribution prepared in the same way. Not only the focal conic texture indicative of the smectic phase can be observed in the micrograph as clearly as in low molecular weight smectic liquid crystals, but also that the small-angle X-ray scattering pattern (Fig. 17.2c) revealed smectic layer reflections on the meridional line in the orientation direction (Okoshi et al. 2010). These reflections are perpendicular to the several reflections on the equatorial line in the wide-angle X-ray scattering pattern (Fig. 17.2d), which are assigned to the two-dimensional

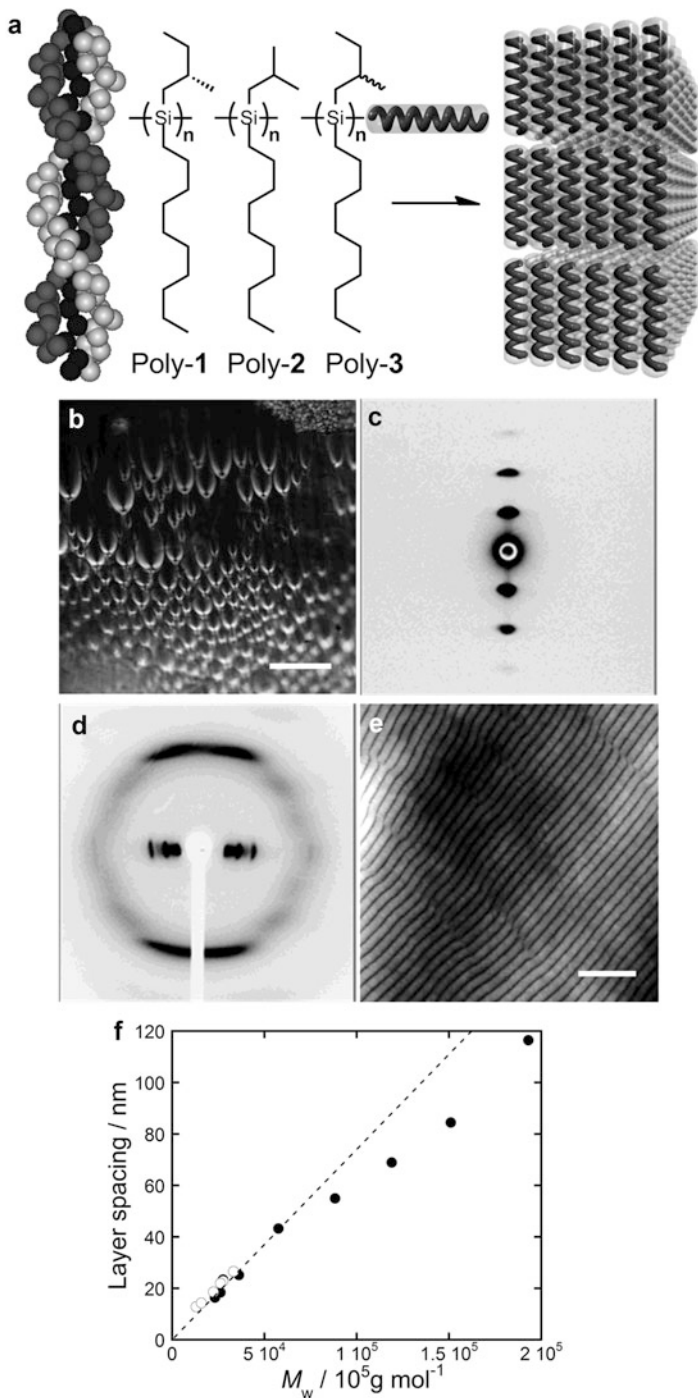


Fig. 17.2 (a) Illustrations of the structures of polysilanes and their smectic liquid crystal formation. (b) Polarizing optical microscopic image of poly-1 (scale bar: 100 μm). (c) Small- and (d) wide-angle X-ray diffraction patterns of poly-3 (Okoshi et al. 2010). (e) AFM phase image observed on the cast film of poly-2 (scale bar: 200 nm). (f) Smectic layer spacings observed in poly-2 along with small-angle X-ray diffractions (open squares) and AFM (closed circles) (Oka et al. 2008)

orthogonal lattice of the lateral polymer packing (Okoshi et al. 2002a). This is clear evidence of the apparent smectic B phase where molecules oriented perpendicular to the smectic layers are arranged in a close-packed lattice. This smectic layer can also be directly observed by atomic force microscopy (AFM) as shown in Fig. 17.2e. The AFM image was taken on the top surface of a 1- μm thick cast film of polysilane on a glass substrate after annealing in saturated solvent vapor (Oka et al. 2008). The observed banding pattern is so regular that its correlation length seemingly extends beyond the microscopic field of view although the molecular distribution in smectic layers is generally described as sinusoidal in liquid crystal textbooks. The observed banding repeats, which is over 200 nm at most, far beyond its persistence length, were plotted as closed circles versus the molecular weight, while the smectic layer spacings obtained from the X-ray diffraction were plotted as open circles in Fig. 17.2f (Oka et al. 2008). Most of the plots are on the dotted line which represents the polymer length calculated from $1.96 \text{ \AA} (\text{unit translation}) \times n$ (degree of polymerization), although both the theoretical and computational studies predicted that the smectic layer spacings are 1.2–1.4 times longer than the molecular lengths. The further quantitative analysis requires the absolute molecular weight measurements because this might be due to the overestimated molecular weights for stiff polymers measured by size exclusion chromatography (SEC) with polystyrene standard calibrations.

The smectic fan-shaped optical microscopic texture of poly-1 gradually turned into a Grandjean texture with oily streaks characteristic of the cholesteric phase upon heating at around 150 °C (Figs. 17.3a, b) (Okoshi et al. 2004a), although the development of the fan-shaped texture upon cooling can be observed only at the air interface and not in the entire field of view. Almost concurrently, the smectic layer reflection in the small-angle X-ray scattering disappeared (Fig. 17.3d) and a selective reflection band of the cholesteric phase appeared in the CD spectra (Fig. 17.3e) at around the same temperature after the disappearance of the reflections from the two-dimensional lattice of the lateral polymer packing in the wide-angle X-ray scattering at the lower temperature upon heating (Fig. 17.3c). These results clearly indicated that poly-1 shows the smectic B—smectic A—cholesteric (chiral nematic) phase transition although it is still unclear whether the smectic B phase corresponds to the predicted smectic phase with the columnar hexagonal lattice in the transverse direction that appeared in the large scale simulation or the non-equilibrium state from the smectic phase to the columnar phase predicted by the small scale simulation (Veerman and Frenkel 1991).

The entire phase diagram of poly-1 was revealed by plotting the phase transition temperature versus the molecular weight (Fig. 17.3f). The cholesteric phase can be observed only with low molecular weight samples because high molecular weight samples start to decompose over 200 °C prior to the phase transition. Poly-2 and 3 also show a similar phase transition behavior except for the nematic phase instead of the cholesteric phase due to a lack of optical activity. While most of the theoretical predictions have been made on athermal lyotropic systems, the phase behavior of polysilane nevertheless reproduced the predicted columnar—smectic—

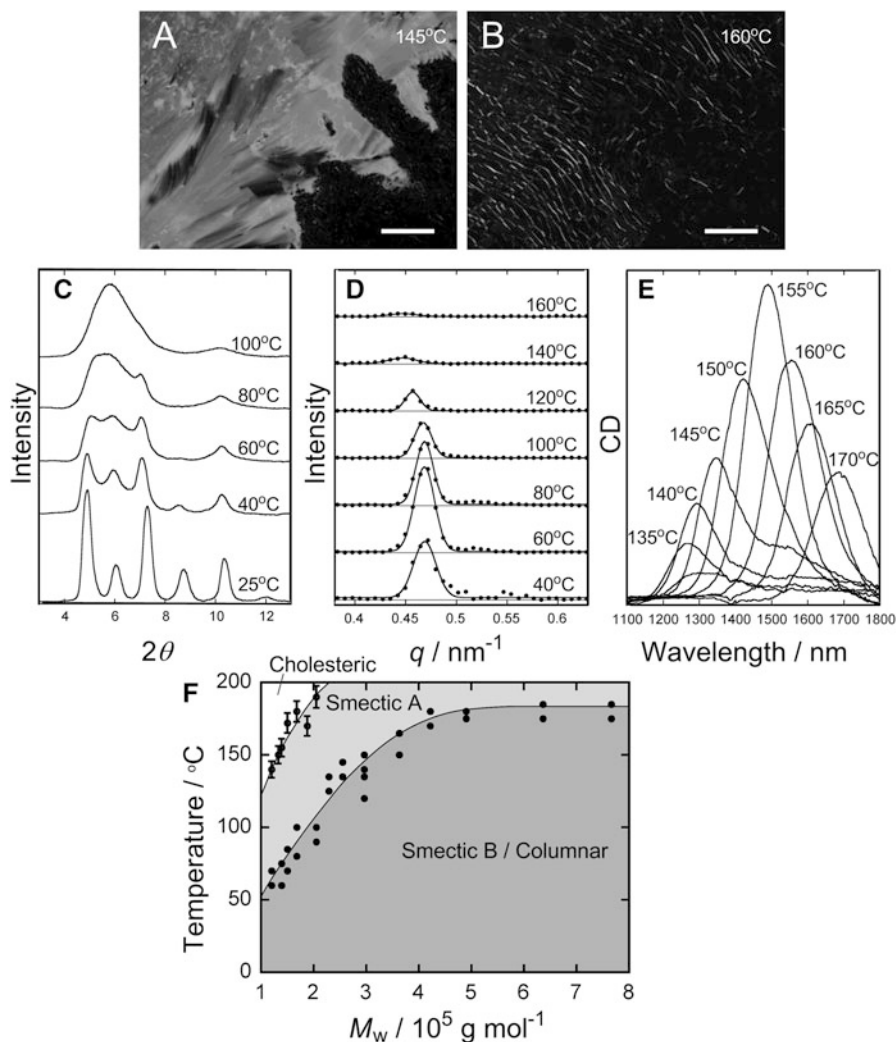


Fig. 17.3 (a, b) Polarizing optical microscopic images (scale bars: 100 μm) (Okoshi et al. 2004a), (c) small-angle, (d) wide-angle X-ray diffraction patterns, and (e) CD spectra of poly-1 taken over the smectic-cholesteric liquid crystal phase transition temperature. (f) Phase diagram of poly-1 as a function of the molecular weight and temperature

nematic liquid crystal phase sequence when the decrease in the reduced volume density is taken as the increase in temperature.

Similar results have been reported with polypeptide (Okoshi et al. 2002b) and polyisocyanide (Onouchi et al. 2008). The polyisocyanide has an extremely stiff backbone with the persistence length of 220 nm due to the tight intramolecular hydrogen bonding networks between the neighboring side chains (Fig. 17.4)

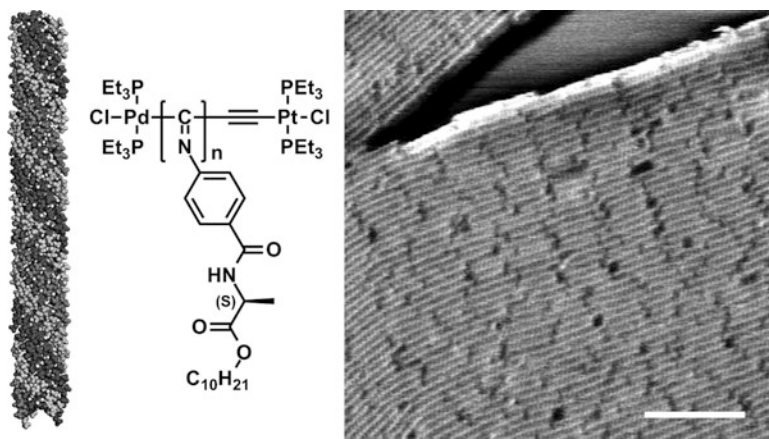


Fig. 17.4 Structure of the polyisocyanide and AFM image showing the molecular arrangement within the smectic layers (scale bar: 30 nm) (Onouchi et al. 2008)

(Okoshi et al. 2008), which makes it possible to visualize the molecular arrangement within the smectic layers by AFM observations. The observed AFM image in Fig. 17.4 shows how polymers with a length polydispersity beyond the predicted limit of $M_w/M_n = 1.03$ are packed within a layer to extend the correlation length of the smectic layers. The polymers with different lengths are seemingly arranged within a layer in such a manner that the concavity and convexity of the layers match between the layers to align the center of gravity of the polymers within the layer, which is the only way to maintain the layer structure even with the length polydispersity of the component. This result is also supported by X-ray structural analyses of the smectic layers in the phase transition process (Okoshi et al. 2004b).

17.3 Smectic Phases of Binary Mixtures of Rod-Like Polymers

17.3.1 Theoretical Predictions

In order to assess the effect of the length polydispersity on the liquid crystal phase formation, binary mixtures of rod-like particles with different lengths have been computed because novel incommensurate smectic phases can be expected to fit together the smectic layers with different layer spacings, although it is intuitively understandable that the length polydispersity of the rod-like particles hampers the smectic phase formation because it is difficult for rods with different lengths to fit in the same smectic layer.

Koda et al. performed a theoretical study of the binary system of rod-like particles with different lengths using the mean field approximation to predict the formation of three types of smectic phases (Koda and Kimura 1994). That is to say, by adding a small fraction of shorter rods to longer rods, both the short and long rods are mixed within a smectic layer if the length ratio is below 2.5. However, smectic layers of short rods are alternately stacked with that of the long rods when the length ratio is over 2.5, and these are segregated from each other with the length ratio over 5.0. Varga et al. predicted four different types of smectic phases (see Fig. 17.5)

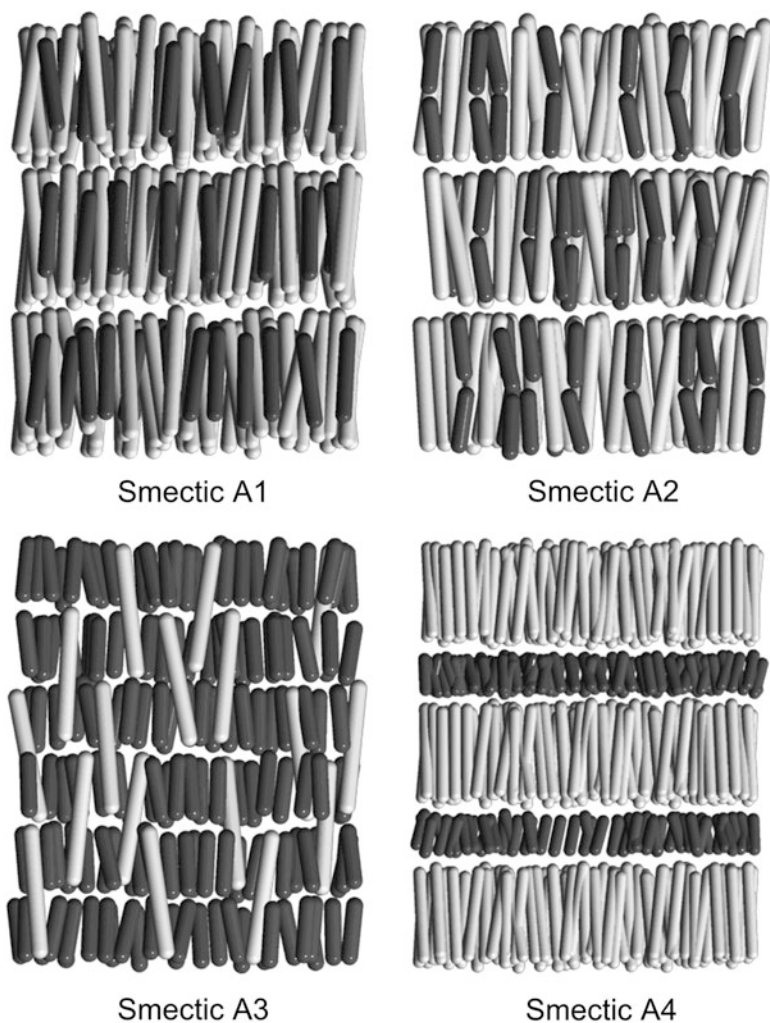


Fig. 17.5 Illustrations of four predicted different types of smectic phases in the binary mixture of rod-like particles with different lengths

depending on the mixing ratio and the length ratio of the short and long rods in the binary mixture of rod-like particles: (1) short and long rods with the length ratio of 1.5 are mixed within the same smectic layer regardless of the mixing ratio (called this smectic A1 for the sake of expediency); (2) a smectic layer of long rods accommodates two smectic layers of short rods in the mixture of scarce short rods and abundant long rods with the length ratio of 2.0 (smectic A2); (3) long rods randomly straddle a pair of smectic layers of short rods in the mixture of abundant short rods and scarce long rods with the length ratio of 2.0 (smectic A3), even though the smectic phase is destabilized between smectics A2 and A3; and (4) smectic layers of short rods and smectic layers of long rods alternately stacked in the mixture of scarce short rods and abundant long rods with the length ratio of 3.3 (smectic A4), which is destabilized and turns into the nematic phase with abundant short rods and scarce long rods (Varga et al. 2009; Varga and Velasco 2010).

These somewhat surprising predictions, however, had never been verified because there have been no appropriate experimental systems of rod-like particles with freely adjustable lengths.

17.3.2 *Experimental Verifications*

The structural analyses of the smectic phases in the binary mixture of polysilanes with different molecular weights have been performed and provided an answer to this question. The observed layer spacings in the X-ray diffractions of the binary mixtures (normalized by the layer spacings of the short polymers) at the mixing ratio of 0.75 (weight of long polymer / weight of binary mixture) were plotted versus the molecular weight ratios (long polymer / short polymer, which should be the length ratio) in Fig. 17.6 (Okoshi et al. 2009). When the molecular weight ratio is relatively low (<1.7), only one reflection is observed whose spacing corresponds to the average molecular length (solid line in Fig. 17.6), assuming that both are completely mixed within a layer. Thus, the structure of smectic A1 is formed in this range of molecular weight ratios. In contrast, with a higher molecular weight ratio (>1.7), they show two reflections with the larger spacing twice as long as the shorter one, regarded as the first and second order reflections. However, with the decreasing mixing ratio of the long polymer, only the first order reflection disappeared and the second order reflection remained. The only plausible explanation for this is the conversion from smectic A2 to smectic A3 because the second order reflection, intensified by the low electron density part at the center of the smectic layer of long polymer, should turn into the smectic layer reflection of smectic A3 after the long polymer smectic ordering disappeared upon adding the short polymer. These characteristic smectic layer structures were confirmed by the AFM observations. Figure 17.7 shows the AFM images of the binary mixtures with the molecular weight ratio of 2.49 and varying mixing ratios (Okoshi et al. 2009). The bandings observed in the long polymer (Fig. 17.7a), which are characteristic of repeating smectic layers, are found to split into two narrow bandings upon adding

Fig. 17.6 Layer spacings observed in the binary mixtures with the mixing ratio of 0.75 plotted versus the molecular weight ratio. Layer spacings are normalized by the layer spacings observed in each of the short polymers, which are represented by the *circles, squares, triangles, and diamonds* (Okoshi et al. 2009)

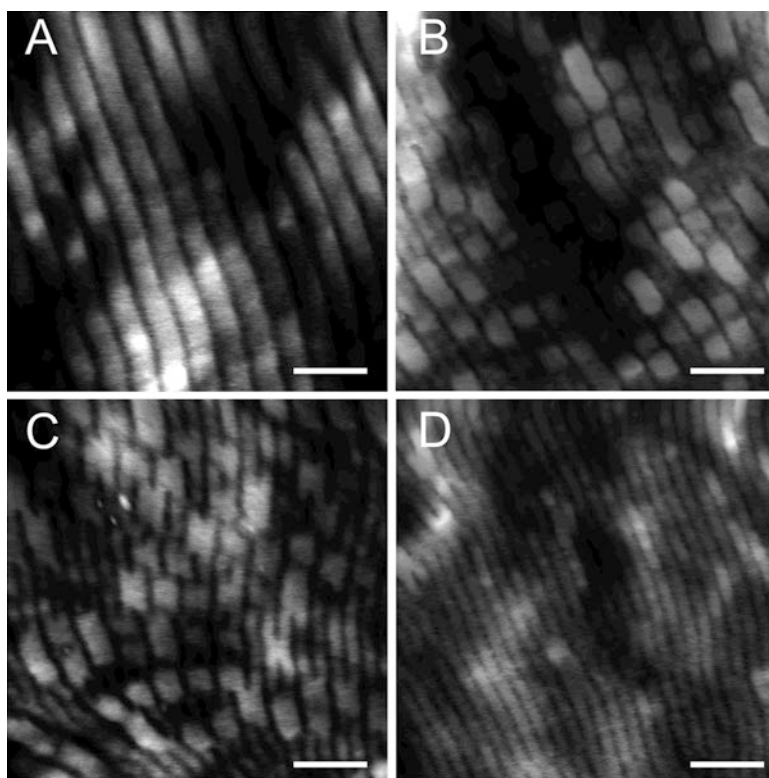
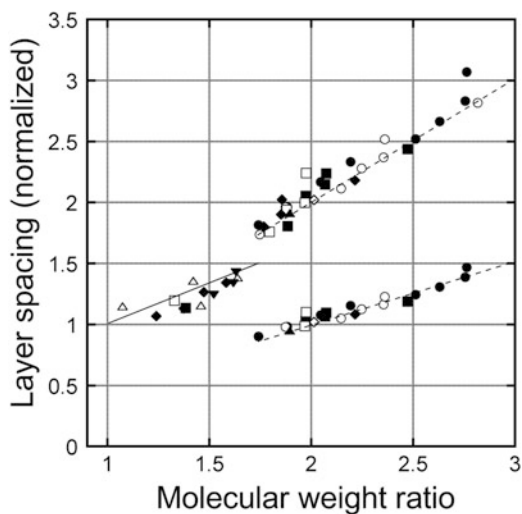


Fig. 17.7 AFM images of the binary mixtures (molecular weight ratio: 2.49) of poly-1 with the mixing ratios of (a) 1.00, (b) 0.75, (c) 0.5, (d) 0.33 (scale bars: 200 nm) (Okoshi et al. 2009)

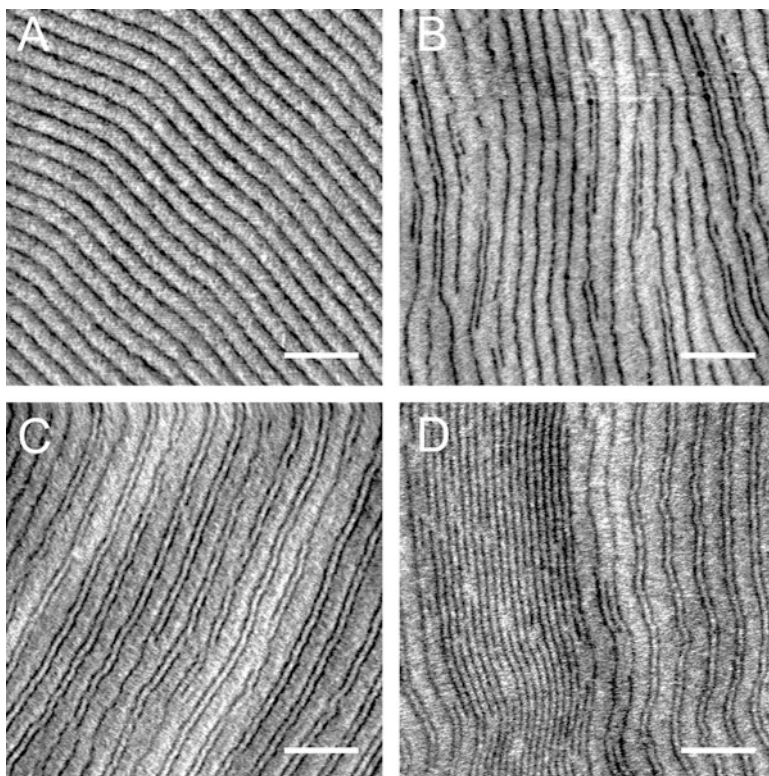


Fig. 17.8 AFM images of the binary mixtures (molecular weight ratio: 3.14) of poly-2 with the mixing ratios of (a) 1.00, (b) 0.83, (c) 0.75, (d) 0.50 (scale bars: 400 nm) (Okoshi and Watanabe 2010)

the short polymer (Fig. 17.7b), come out of alignment occasionally by a half pitch of wide bandings (Fig. 17.7c) upon further addition, and finally turn into narrow bandings with the wide bandings disappearing (Fig. 17.7d). These AFM images are clearly visualizing the conversion from the smectic A2 with two smectic layers of short polymers nested in a smectic layer of long polymers (Fig. 17.7b) to the smectic A3 probably with the long polymers randomly straddling the two smectic layers of short polymers (Fig. 17.7d) via a frustrated phase (Fig. 17.7c) upon decreasing the mixing ratio of the long polymer, even without showing the nematic phase predicted between smectics A2 and A3.

For a higher molecular weight ratio, the AFM observations have also been performed in the same manner. Figure 17.8 shows the AFM images of the binary mixtures with the molecular weight ratio of 3.14 and varying mixing ratio (Okoshi and Watanabe 2010). Upon adding the short polymer to the long polymer, these samples did not show the smectic A2, but showed that a single smectic layer for the short polymer was occasionally inserted between the smectic layers of the long polymer (Figs. 17.8a, b) at the long polymer mixing ratio of 0.87. By further

increasing the short polymer, this allowed the complete alternating stacking of the narrow smectic layer for the short polymer and wide smectic layers of the long polymer at the long polymer mixing ratio of 0.75, almost perfectly reproducing the predicted smectic A4 (Fig. 17.8c). Upon further adding of the short polymer, the excess short polymer was ejected from the smectic A4 and formed smectic layers in its pure form, which is not a discontinuous phase separation, but segregation between the smectic layers of smectic A4 in a parallel manner. These are contrary to the prediction in which the smectic A4 would be destabilized and less favored than the nematic phase when the short rod is abundant. The smectic phase is more preferred than predicted, which might be due to the fact that it is irrelevant to apply the theories with no intermolecular attraction taken into consideration to the dense thermotropic real system.

17.4 Conclusion

The liquid crystal properties of countless numbers of molecules have been studied and classified in terms of the types of liquid crystal structures which is strongly influenced by their chemical structural properties. Distracted by these rich and abundant variety of liquid crystals due to the innumerable chemical structures of the liquid crystalline molecules, the essential quality of liquid crystal formation, which has been merely predicted in the theoretical studies of rod-like particle systems, has failed to be understood because these coarse-grained models have not duplicated the real molecular systems in the experimental point of view. We have presented here the smectic phases formed in rod-like helical polymer systems which is almost the perfect model for the verification of these theoretical predictions. Although these polymers are simple homopolymers, which behave as simple rod-like particles, they show truly colorful liquid crystalline behaviors whose origins are clear due to their structural simplicity. The development of liquid crystalline polymer systems and the verification of the preceding predictions are just beginning and may become a wider research field both to determine the origin of the liquid crystalline behavior and to develop novel polymer materials.

References

- Adams M, Dozic Z, Keller SL, Fraden S (1998) Entropy driven microphase transition in mixtures of colloidal rods and spheres. *Nature* 393:349–352
- Bates MA, Frenkel D (1998) Influence of polydispersity on the phase behavior of colloidal liquid crystals: a Monte Carlo simulation study. *J Chem Phys* 109:6193–6199
- Bolhuis P, Frenkel D (1997) Tracing the phase boundaries of hard spherocylinders. *J Chem Phys* 106:666–687
- Dozic Z, Fraden S (1997) Smectic phase in a colloidal suspension of semiflexible virus particles. *Phys Rev Lett* 78:2417–2420

- Flory PJ (1956) Phase equilibria in solutions of rod-like particles. *Proc Roy Soc Ser A* 243:73–89
- Frenkel D, Moulder BM, McTague JP (1984) Phase diagram of a system of hard ellipsoid. *Phys Rev Lett* 52:287–290
- Fujiki M (1996) A correlation between global conformation of polysilane and UV absorption characteristics. *J Am Chem Soc* 118:7424–7425
- Gabriel J-CP, Camerel F, Lemarie BJ, Desvaux H, Davidson P, Batail P (2001) Swollen liquid-crystalline lamellar phase based on extended solid-like sheet. *Nature* 413:504–508
- He S-J, Lee C, Gido SP, Yu SM, Tirrell DA (1998) A twist boundary-like twisted smectic phase in monodisperse poly(γ -benzyl α , L-glutamate) produced by recombinant DNA techniques. *Macromolecules* 31:9387–9389
- Hosino M, Nakano N, Kimura H (1979) Nematic-smectic transition in an aligned rod system. *J Phys Soc Jpn* 46:1709–1715
- Hosino M, Nakano N, Kimura H (1982) Phase transitions in the systems of identical rigid molecules in perfect alignment—relations of the smectic A and columnar ordering in liquid crystals and the crystalline orderings to the molecular shape. *J Phys Soc Jpn* 51:741–748
- Kobayashi KK (1970) Theory of translational and orientational melting with application of liquid crystals. I. *J Phys Soc Jpn* 29:101–105
- Koda T, Kimura H (1994) Phase diagram of the nematic-smectic A transition of the binary mixture of parallel hard cylinders of different lengths. *J Phys Soc Jpn* 62:984–994
- Lee S-W, Mao C, Flynn CE, Belcher AM (2002) Ordering of quantum dots using genetically engineered viruses. *Science* 296:892–895
- Lee S-W, Wood BM, Belcher AM (2003) Chiral smectic C structure of virus-based film. *Langmuir* 19:1592–1598
- Li L, Walda J, Manna L, Alivisatos AP (2002) Semiconductor nanorod liquid crystals. *Nano Lett* 2:557–560
- Livolant F, Bouligand Y (1986) Liquid crystalline phases given by helical biological polymers (DNA, PBLG and xanthan). Columnar textures. *J Phys* 47:1813–1827
- McMillan WL (1971) Simple molecular model for the smectic A phase of liquid crystals. *Phys Rev A* 4:1238–1246
- Michael PA (1990) Computer simulation of a biaxial liquid crystal. *Liq Cryst* 8:499–511
- Oka H, Suzaki G, Edo S, Suzuki A, Tokita M, Watanabe J (2008) Structural characteristics of thermotropic smA layer phase formed from rigid-rod polysilanes. *Macromolecules* 41:7783–7786
- Okoshi K, Watanabe J (2010) Alternating thick and thin layers observed in the smectic phase of binary mixtures of rigid-rod helical polysilanes with different molecular lengths. *Macromolecules* 43:5177–5179
- Okoshi K, Kamee H, Suzaki G, Tokita M, Fujiki M, Watanabe J (2002a) Well-defined phase sequence including cholesteric, smectic A, and columnar phases observed in a thermotropic LC system of simple rigid-rod helical polysilane. *Macromolecules* 35:4556–4559
- Okoshi K, Sano N, Suzaki G, Tokita M, Magoshi J, Watanabe J (2002b) Smectic liquid crystal observed in thermotropic system of rigid-rod poly(γ -octadecyl-L-glutamate). *Jpn J Appl Phys* 41:L720–L722
- Okoshi K, Saxena A, Naito M, Suzaki G, Tokita M, Watanabe J, Fujiki M (2004a) First observation of a smectic A-cholesteric phase transition in a thermotropic liquid crystal consisting of a rigid-rod helical polysilane. *Liq Cryst* 31:279–283
- Okoshi K, Saxena A, Fujiki M, Suzaki G, Watanabe J, Tokita M (2004b) Small-angle X-ray analysis of smectic A cholesteric liquid crystal phase transition in rigid-rod helical polysilane. *Mol Cryst Liq Cryst* 418:57–68
- Okoshi K, Nagai K, Kajitani T, S-I S, Yashima E (2008) Anomalous stiff backbones of helical poly(phenyl isocyanide) derivatives. *Macromolecules* 41:7752–7754
- Okoshi K, Suzuki A, Tokita M, Fujiki M, Watanabe J (2009) Entropically-driven formation of smectic A1, A2, and A3 phases in binary mixtures of rigid-rod helical polysilanes with different molecular weights. *Macromolecules* 42:3443–3447

- Okoshi K, Hagihara T, Fujiki M, Watanabe J (2010) Anomalous thermotropic liquid crystalline phase behavior in poly [*n*-decyl-(*RS*)-2-methylbutylsilane]s with narrow molecular weight distributions. *Liq Cryst* 37:1183–1190
- Onouchi H, Okoshi K, Kajitani T, S-i S, Nagai K, Kumaki J, Onitsuka K, Yashima E (2008) Two- and three-dimensional smectic ordering of single-handed helical polymers. *J Am Chem Soc* 130:229–236
- Onsager L (1949) The effect of shapes on the interaction of colloidal particles. *Ann N Y Acad Sci* 51:627–659
- Stroobants A, Lekkerkerker HNW, Frenkel D (1987) Evidence for one-, two-, and three-dimensional order in a system of hard parallel spherocylinders. *Phys Rev A* 36:2929–2945
- Strzelecka TE, Davidson MW, Rill LR (1988) Multiple liquid crystal phases of DNA at high concentrations. *Nature* 331:457–460
- Terao K, Terao Y, Teramoto A, Nakamura N, Terakawa I, Sato T (2001) stiffness of polysilanes depending remarkably on a subtle difference in chiral side chain structure: Poly{*n*-hexyl-[(*S*)-2-methylbutyl]silane} and poly{*n*-hexyl-[(*S*)-3-methylpentyl]silane}. *Macromolecules* 34:2682–2685
- Varga S, Velasco E (2010) Modeling and understanding smectic-phase formation in binary mixtures of rodlike polysilane: comparison of Onsager theory and experiment. *Macromolecules* 43:3956–3963
- Varga S, Velasco E, Mederos L, Vesely FJ (2009) Stability of the columnar and smectic phases of length-bidisperse parallel hard cylinders. *Mol Phys* 107:2481–2492
- Veerman JAC, Frenkel D (1991) Relative stability of columnar and crystalline phases in a system of parallel hard spherocylinders. *Phys Rev A* 43:4334–4343
- Veerman JAC, Frenkel D (1992) Phase behavior of disk-like hard-core mesogens. *Phys Rev A* 45:5632–5648
- Watanabe J, Takashina Y (1992) Thermotropic polypeptides VIII. Anomalous phase behavior in low molecular-weight poly(γ -octadecyl L-glutamate). *Polymer J* 24:709–713
- Wen X, Meyer RB, Casper DLD (1989) Observation of smectic-A ordering in a solution of rigid-rod-like particles. *Phys Rev Lett* 63:2760–2763
- Yu SM, Conticello VP, Zhang G, Kayser C, Fournier MJ, Mason TL, Tirrell DA (1997) Smectic ordering in solutions and films of a rod-like polymer owing to monodispersity of chain length. *Nature* 389:167–170
- Zhang G, Fournier MJ, Mason TL, Tirrell DA (1992) Biological synthesis of monodisperse derivatives of poly(α , L-glutamic acid): model rod-like polymers. *Macromolecules* 25:3601–3603